Electronic Supplementary Material (ESI) for Energy & Environmental Science

SUPPLEMENTARY INFORMATION

Reversible CO_2 Capture with Porous Polymers using the Humidity Swing

*Hongkun He,[1] Wenwen Li,[1] Mingjiang Zhong,[1] Dominik Konkolewicz,[1] Dingcai Wu,[2] Karin Yaccato,[3] Tim Rappold,[3] Glenn Sugar,[3] Nathaniel E. David,[3] and Krzysztof Matyjaszewski[1]**

[1]Department of Chemistry, Carnegie Mellon University, 4400 Fifth Avenue, Pittsburgh, Pennsylvania 15213, USA

[2]Materials Science Institute, Key Laboratory for Polymeric Composite and Functional Materials of Ministry of Education, School of Chemistry and Chemical Engineering, Sun Yat-sen University, Guangzhou 510275, P. R. China

[3]Kilimanjaro Energy, Inc., 630 Tennessee Street, San Francisco, California 94107, USA

E-mail: km3b@andrew.cmu.edu

Supplementary Information contains:

Supplementary Methods

Materials

Excellion membrane I-200 (SnowPure LLC, CA) and Excellion active resin (Purolite CO, PA) were exchanged to the hydroxide form according to the procedures described elsewhere.[1] Carbon black (Monarch 700) was supplied by Cabot Corp. (Billerica, MA). Sodium azide (≥99.5%), phosphorus tribromide (PBr_3, 99%), trimethylamine solution (31-35 wt. % in ethanol, ~4.2 M), α,α'-dichloro-*p*-xylene (98%), (vinylbenzyl)trimethylammonium chloride (VBTMACl, 99%), methyl methacrylate (MMA) (≥98.5%), Span 80, potassium persulfate (KPS), potassium sulfate (K_2SO_4), *N*,*N*-dimethyl formamide (DMF) and *N,N,N',N'',N''*-pentamethyldiethylenetriamine (PMDETA, 99%) were purchased from Aldrich. 4-Vinylbenzyl chloride (or *p*-chloromethylstyrene, CMS, ≥90%) and divinylbenzene (DVB) were purchased from Aldrich and purified by passing over a column of basic alumina to remove the inhibitor, then stored at -5 ℃. CuCl and $CuCl_2$ were purchased from Aldrich in the highest available purity. Potassium hydroxide (KOH, ≥85.0%), dichloromethane (CH_2Cl_2, 99.9%), ethyl acetate (EtOAc) and water were purchased from Fisher Scientific. Hexane was obtained from Pharmco Aaper. *N*-(4-vinylbenzyl)-*N*,*N*-dimethylamine (90%) was purchased from Acros Organics. 2,2'-Azobis(2-amidinopropane) dihydrochloride (V50) and 2,2'-azobis[2-(2-imidazolin-2-yl)propane]dihydrochloride (VA-044) were purchased from Wako Pure Chemical Industries Ltd. Silica nanoparticle suspension (30 wt% silica in methyl isobutyl ketone, effective diameter D = 20 nm, MIBK-ST) was kindly donated by Nissan Chemical. Hydrophobic groups were then introduced to the silica nanoparticles through the reaction between 1-(chlorodimethylsilyl)propyl 2-bromoisobutyrate with the hydroxyl groups on the silica particle surface according to the previously published procedures.[2] Unless otherwise specified all reagents were used as received.

Instrumentation

All nuclear magnetic resonance (NMR) measurements were performed on a Bruker Avance 300 MHz spectrometer. Thermogravimetric analysis (TGA) was obtained on a TG/DTA6300 analyzer (Seiko Instruments, Inc.) under a N_2 atmosphere (flow rate 50 mL/min). Elemental analyses were performed on an Exeter Analytical CE440 elemental analyser in Midwest Microlab, LLC. Scanning electron microscopy (SEM) analysis was conducted using a Hitachi 2460N scanning electron microscope. The specimens were attached to SEM stubs using rubber cement or double stick tape, and coated with gold using a Pelco SC-6 sputter coater. Digital images were obtained using Quartz PCI Image management system software. Transmission electron microscopy (TEM) analysis was conducted using a Hitachi H-7100 transmission electron microscope (Hitachi High Technologies America) operating at 75 kV. A small drop of solution containing the sample was placed on a carbon or formvar coated copper grid. After several seconds, the drop was allowed to evaporate or was removed by blotting with filter paper. The sample that remained on the grid was allowed to dry before inserting the grid into the microscope. Digital images were obtained using AMT Advantage 10 CCD Camera System and NIH Image software. The pore structures of all samples were assessed from the N_2 isotherm curve measured by a gas adsorption analyzer (NOVA2000 series, Quantachrome Instruments). Prior to the nitrogen sorption experiments, all samples were degassed at 70 ℃ for at least 24 h to eliminate the surface contaminants (water or oils). The standard analysis of nitrogen sorption isotherms recorded for all samples studied provided the Brunauer-Emmett-Teller (BET) surface area, S_{BET}, evaluated in the range of relative pressure between 0.04-0.2. CO_2 absorption and desorption kinetics were measured using a combination of a Licor, LI-840 infrared analyzer, KNF NMP015M gas pump, Swagelok SS-BNS4-C valves Custom Thermoelectric coolers and aluminum blocks designed to control the humidity in the chamber. Nanoscale 3D X-ray microscopy (XRM) was performed using an Xradia UltraXRM-L200 X-ray microscope (Xradia, Inc., Pleasanton, CA, USA). This system incorporates an array of X-ray optical elements to achieve spatial resolutions down to 50 nm, with isotropic voxel dimensions extending to 16 nm × 16 nm × 16 nm. This imaging resolution, previously only achievable with synchrotron beamline sources, has been successfully extended to use with a laboratory X-ray source. The basic construct of a

nanoscale X-ray microscope shares some principles from a transmission optical or electron microscope, incorporating both condenser and objective lenses to project an image onto a CCD detector. However, X-ray focusing elements differ somewhat from their electron and light optical counterparts. An efficient capillary condenser lens provides the initial focusing, while high spatial resolution is realized through the use of Fresnel zone plate objective lenses. These optics are paired with a laboratory rotating-anode X-ray source utilizing a Cu target, producing a quasi-monochromatic X-ray illumination operating at ~ 8.0 keV. Insertion of a gold annulus between the objective zone plate and detector enables Zernike phase contrast imaging, for detection of low-Z features and interfaces.[3] A sequence of 2D radiographs was acquired on the UltraXRM-L200 by rotating the sample through 180 °, pausing at 361 discrete, equally-spaced angular positions to collect a 150 sec view at each step. The resulting series of radiographs was subsequently reconstructed using the Xradia XMReconstructor software package to produce a stack of virtual slices, each with a voxel size of 32 nm × 32 nm × 32 nm. After reconstruction, the virtual slice stack was visualized using both the Xradia XM3DViewer application as well as Avizo® Fire (Visualization Sciences Group, Bordeaux, France).

Preparation of samples for CO_2 absorption/desorption measurements

Excellion membrane and Excellion active resin exchanged to the hydroxide form were cut to the weight desired. The carbon black, colloidal crystal and HIPE based materials were made on the 5-50 mg scale, which were ground by hand using a porcelain mortar and pestle. The material was attached to a standard glass slides (75×25×1 mm) using two sided scotch tape of a known total area. The weight of the glass slide plus tape was determined. Powdered sample (post grinding) was applied to the tape and spread to cover the entire area of the tape surface. Excess powder not adhering to the tape surface was removed. The glass slide plus tape plus powder was weighed, to determine the final weight of the powder alone, and the glass slide was placed in the sample chamber for CO_2 absorption and desorption measurements.

Measurement of samples for CO_2 absorption and desorption

The experimental device shown in Scheme S1 consisted of an infrared gas analyzer, two diaphragm gas pumps, a custom sample chamber, a temperature controlled chamber, a 1.0 μm PTFE filter, and two bellows-sealed pneumatically actuated valves, all connected with ¼" Bevaline IV. The temperature control chamber was made from an aluminum block with a pathway for gas to pass through and a thermocouple placed in the path of the gas. Two thermoelectric coolers (TECs) were secured on the top and bottom of the block. In order to cool the TECs, water circulated through aluminum blocks placed on the outside of the TECs. The dew point, and therefore the humidity, of the system was controlled by placing 1 mL of deionized water in the temperature control chamber and using the TECs to cool the chamber to below room temperature. Temperatures of -2 and 15 ℃ were used to achieve absolute humidity of 5 and 20 ppt, corresponding to 20 and 95% relative humidity, respectively.

The valves were used to purge the system with outside air in order to saturate a sample with CO_2 at low humidity. Typically, samples were at equilibrium with a humidity > 5 ppt before they were placed in the sample chamber. When exposed to the lower humidity (5 ppt) in the system, the samples would start capturing CO_2 from the gas phase, bringing the concentration well below 400 ppm. To replace the CO_2 in the gas phase, the valves would open and the gas pump would turn on, forcing outside air with ~400 ppm CO_2 into the system.

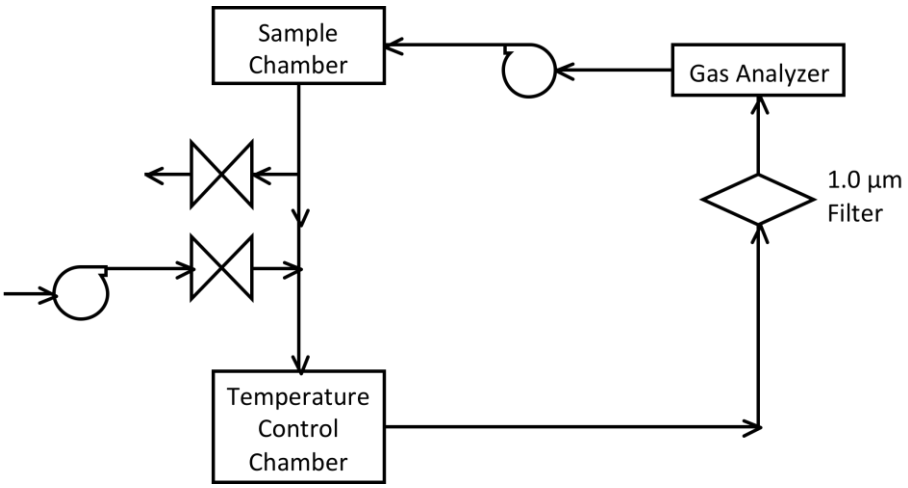

Scheme S1. Experimental setup for the measurement of CO_2 absorption and desorption.

The kinetics of the humidity swing was examined by cycling the water vapor concentrations inside a closed volume between a low level (ca. 5 parts per thousand) and a high level (ca. 20 parts per thousand). High humidity favored relatively high concentrations of CO_2 in the gas phase and low concentrations on the solid sample, while low humidity favored the reverse. The humidity rapidly varied between these two states, followed by a period of time when the humidity was kept constant, to characterize rate at which the CO_2 concentration approached equilibrium. A swing to high humidity thus affected a characteristic rate of CO_2 desorption, while a swing to low humidity yielded a characteristic rate of CO_2 adsorption. The rates were calculated by examining the characteristic slope of the CO_2 concentration vs time profiles, by measuring the average CO_2 change on the middle third of the total CO_2 change induced in a given swing. The changes in CO_2 partial pressure in ppm were converted to molar values, using the known volume of the system.

Synthesis of 1-azidomethyl-4-vinyl-benzene[4]

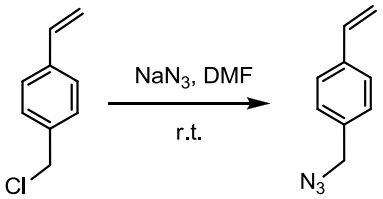

Sodium azide (13.0 g, 0.2 mol), water (75 mL), DMF (250 mL), and 4-vinylbenzyl chloride (15.26 g, 0.1 mol) were added to a flask containing a stir bar. The resulting solution was stirred 48 h at room temperature under a nitrogen atmosphere. The reaction was then diluted with CH_2Cl_2 (100 mL) and poured onto water (400 mL). The layers were separated and the aqueous layer was extracted with CH_2Cl_2. The combined organic layers were then washed with brine, dried over $MgSO_4$, and concentrated by rotary evaporation. The crude material was purified by silica chromatography using 1:9 EtOAc:hexane as eluent and concentrated by rotary evaporation to give 1-azidomethyl-4-vinyl-benzene. ^{1}H NMR ($CDCl_3$, δ, ppm): 4.35 (s, 2H, N_3CH_2), 5.30 and 5.79 (d, 2H, CH_2=CH), 6.74 (m, 1H, CH_2=C*H*), 7.3-7.5 (m, 4H, benzene-*H*).

Synthesis of 1-(azidomethyl)-4-(1-bromoethyl)benzene[5]

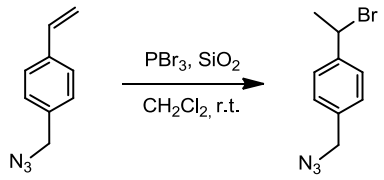

To a stirred suspension of 1-azidomethyl-4-vinyl-benzene (1.59 g, 10 mmol) and SiO_2 (5 g) in CH_2Cl_2 (25 mL), a solution of PBr_3 (1.08 g, 4 mmol) in CH_2Cl_2 (10 mL) was added over 10 min at r.t. The suspension was subsequently stirred for 30 min and then filtered. The SiO_2 was washed with CH_2Cl_2 (15 mL), and the combined organic phase was washed with $NaHCO_3$, then brine, and the organic extract was dried over anhydrous Mg_2SO_4. The solvent was evaporated in a rotatory evaporator at reduced pressure to give 1-(azidomethyl)-4-(1-bromoethyl)benzene. The infrared spectrum shows a strong characteristic absorption peak of azide at 2102 cm^{-1}. ^1H NMR ($CDCl_3$, δ, ppm): 2.07 (d, 3H, CCH_3), 4.36 (s, 1H, N_3CH_2), 5.23 (m, 1H, $CHCH_3$), 7.3-7.5 (m, 4H, benzene-*H*).

Synthesis and characterization of bromine group modified carbon black (CB-N-Br)

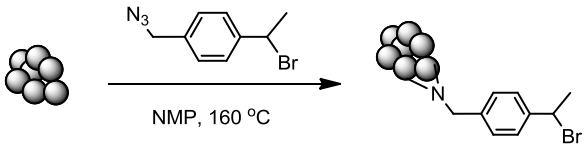

Pristine carbon black (0.25 g) and N-methyl-2-pyrrolidinone (NMP, 20 mL) were placed in a 50 mL Schlenk flask fitted with a condenser. The mixture was ultrasonicated for 1 h and then stirred. 1-(Azidomethyl)-4-(1-bromoethyl)benzene (2.50 g, 10.4 mmol) was added, and the mixture was bubbled with nitrogen for 30 min. The reaction mixture was heated to 160 ℃ for 18 h with constant stirring. After cooling down to room temperature, the product was isolated by precipitation into acetone. The resulting precipitate was redispersed in acetone using ultrasonication and then collected by centrifugation. This process was repeated until the upper layer was nearly colorless. The separated solid was sequentially redispersed in water and purified by at least five centrifugation cycles, and then

redispersed in acetone and purified by three centrifugation cycles. The supernatant was decanted and the black solid was dried under vacuum at 60 ^{o}C overnight to give CB-N-Br. The Br content in CB-N-Br is 14.74 wt% determined by elemental analysis, which corresponds to 1.84 mmol/g.

Synthesis of dicationic crosslinker (PMVPMACl)

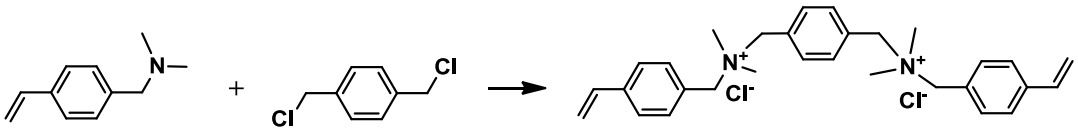

α,α'-Dichloro-p-xylene (9.50 g, 0.0543 mol) was added to methanol (27.0 mL) in a 100 mL round-bottom flask. *N*-(4-vinylbenzyl)-*N*,*N*-dimethylamine (17.50 g, 0.1085 mol) and deionized water (4.9 mL) were sequentially added. The mixture was heated at 50 ^{o}C for 12 h. After cooling to room temperature, the reaction solution was precipitated into cold acetone (800 mL). The precipite was filtered and washed repeatedly with acetone, and dried *in vacuo* at room temperature. The final product of *N*,*N*'-(1,4-phenylenebis(methylene))bis(*N*,*N*-dimethyl-1-(4-vinylphenyl)methanamonium) dichloride (PMVPMACl) was obtained as white powders (Yield: 83%). (HH-2-82) ^{1}H NMR (D_2O, δ, ppm): 2.94 (s, 12H, C*H*$_3$), 4.56 (d, 8H, NC*H*$_2$), 5.38 and 5.90 (d, 4H, C*H*$_2$=CH), 6.80 (m, 2H, CH$_2$=C*H*), 7.5-7.7 (m, 12H, benzene-*H*).

Preparation of CB-*g*-p(NMe$_3^+$-MS OH$^-$)

The bromine group modified carbon black (CB-N-Br) (100 mg, 0.184 mmol Br) and *N*,*N*-dimethyl formamide (DMF, 5.19 mL) was added into a Schlenk flask and sonicated for 30 min. p-Chloromethylstyrene (CMS, 10.37 mL, 73.6 mmol), $CuCl_2$ (1.2 mg, 0.009 mmol), and *N,N,N',N'',N''*-pentamethyldiethylenetriamine (PMDETA, 38.4 μL, 0.184 mmol) were added. The flask was then degassed by five freeze-pump-thaw cycles. While the contents were frozen, the flask was back filled with nitrogen and CuCl (17.3 mg, 0.175 mmol) was added. The flask was then evacuated and back filled with nitrogen thrice. The flask was allowed to warm up to room temperature and an initial sample was collected. The flask was then placed in an oil bath at 100 ^{o}C for 48 h. The conversion was determined by

^{1}H NMR and found to be 56%, calculated from consumption of double bonds relative to DMF (internal standard). After washing with tetrahydrofuran (THF), the sample was characterized by TGA (see Figure S1).

CB-*g*-CMS (100 mg) was mixed with trimethylamine (35% ethanol solution, 10 mL). The mixture was sonicated and stirred at room temperature for 1 d. The reaction mixture was separated by centrifugation and washed repeatedly with methanol. Then the sample was mixed with KOH (0.2 g/mL aqueous solution, 15 mL) and stirred at room temperature for 1 d. The reaction mixture was separated by centrifugation and washed repeatedly with methanol and dried in vacuum at 50 ^{o}C to give CB-*g*-p(NR_3^+-MS OH^-).

Preparation of Colloidal crystal template p(NMe_3^+-MS OH^-)

The PMMA spheres were synthesized by surfactant-free emulsion polymerization using an optimized version of literature techniques.[6-7] A mixture of water (165 mL) and methyl methacrylate (MMA, 30 mL, 0.28 mol) was prepared in a three-neck round-bottom flask, with a water-cooled condenser. The mixture was stirred at 350 rpm, while being heated to 75 ℃ and purged with nitrogen gas. After stabilization of the temperature at an elevated level, V50 (76 mg, 0.28 mmol) was added, and the reaction was allowed to proceed for 2 h, producing colloidal PMMA spheres. The colloidal polymer was filtered through cotton to remove any large agglomerates. PMMA colloidal crystals were formed by centrifuging the colloid at 1500 rpm for 24 h, decanting the water, and allowing the solid to dry for 3 days.

A solution of (vinylbenzyl)trimethylammonium chloride (VBTMACl, 2.0 g, 11.4 mmol), *N*,*N*'-(1,4-phenylenebis(methylene))bis(*N*,*N*-dimethyl-1-(4-vinylphenyl)methanamonium) dichloride (PMVPMACl, 0.77 g, 2.3 mmol), VA-044 (2.8 mg, 0.01 mmol), and water (1 mL) was prepared. Dried

PMMA colloidal crystals (with average diameter of 480 nm) were crushed to a powder and deposited in millimeter-thick layers on filter paper in a Büchner funnel. With suction applied to the Büchner funnel, the precursor solution was applied dropwise to completely wet the PMMA powder. Equal amounts of PMMA and precursor solution, by mass, were used. The composite sample was placed in an oven at 80 ^{o}C for 18 h. The PMMA template was removed from the sample by extraction for 3 days in a refluxing solution of 1:1 (v/v) THF and acetone in a Soxhlet extractor. The product was dried in vacuum at room temperature overnight.

For the ion-exchange, 0.5 g of the product was added into a KOH methanol solution (0.2 g/mL, 20 mL), and stirred for one day at room temperature, and then separated by filtration and washed with excess methanol until neutral, and finally dried in vacuum at room temperature overnight to give p(NMe_3^+-MS OH^-).

Preparation of HIPE templated p(NMe_3^+-MS OH^-)

The functionalized silica nanoparticles (0.12 g) were dispersed in a mixture of CMS (2.39 g, 15.6 mmol), divinylbenzene (DVB, 0.62 g, 4.7 mmol) and Span 80 (0.3 g, 0.7 mmol) to form the continuous organic phase. Meanwhile, potassium persulfate (KPS, 40 mg, 0.15 mmol) and K_2SO_4 (80 mg, 0.46 mmol) were dissolved in 16.8 g of water to form the dispersed aqueous phase. The aqueous solution was then slowly added to the organic phase under stirring to generate a stable emulsion. The formed HIPE was transferred into free standing polypropylene centrifuge tubes and polymerized at 70 ℃ for 24 h in an oven to yield the porous polymers. The formed porous polymers were purified by Soxhlet extraction first in distilled water followed by acetone for 24 h to remove residual surfactant and finally dried under vacuum.

0.5 g of pCMS prepared by Pickering HIPE polymerization was added to trimethylamine (35% ethanol solution, 30 mL), and the mixture was stirred at 50 ^{o}C for 48 h and then washed with methanol. For the

ion-exchange, 0.5 g of the product was mixed with 30 mL KOH aqueous solution (0.5 g/mL) and stirred overnight at room temperature. The resulting sample was washed extensively with water and methanol and dried under vacuum to give the HIPE templated p(NR_3^+-MS OH^-).

Supplementary Data

Thermogravimetric analysis (TGA) of carbon black grafted material

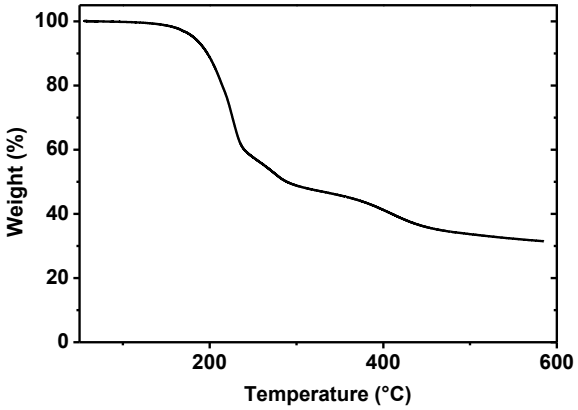

Figure S1. TGA curves of CB-*g*-CMS.

Absorption/Desorption profiles for Excellion Membrane, Excellion Active Resin, carbon black grafted material, colloidal crystal templated material and HIPE templated material.

The absorption/desorption characteristics of the four materials studied are shown below. In all cases the material is first saturated with carbon dioxide, before being exposed to humid conditions to release the carbon dioxide from the material, followed by a reduction in the humidity to trigger the capture of the CO_2. In all cases a low humidity of approximately 5 parts per thousand (ppt) is used, and a high humidity of approximately 20 ppt is used. To determine the characteristic absorption and desorption rates the middle third of the CO_2 swing is used, to minimize the impact of different run times near the equilibrium concentrations. For example, if the initial CO_2 concentration on a desorption swing was 400 ppm, and the final CO_2 concentration was 1,000 ppm, then the average characteristic rate was the CO_2 change per unit time between 600 ppm and 800 ppm. These values in ppm were converted to molar values of CO_2 absorbed or desorbed using the known volume of the system and the ideal gas law.

In the case of Excellion Membrane (Figure S2) the kinetics are very slow with an absorption rate of 4.0 $\times 10^{-3}$ mmol/g/min, a desorption rate of 4.5 $\times 10^{-3}$ mmol/g/min and a swing size of 1.3 $\times 10^{-1}$ mmol/g. Similarly, for the Excellion Active Resin (Figure S3) the kinetics are slow with an absorption rate of 5.4 $\times 10^{-3}$ mmol/g/min, a desorption rate of 1.0 $\times 10^{-2}$ mmol/g/min and a swing size of 1.9 $\times 10^{-1}$ mmol/g.

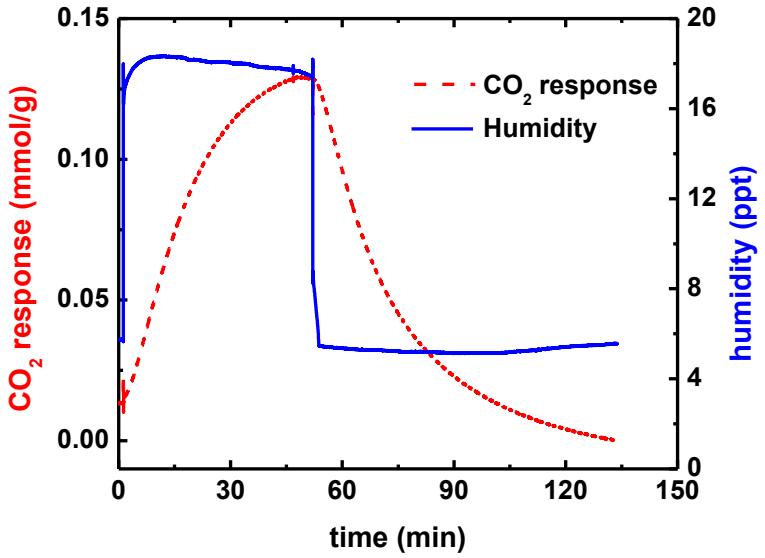

Figure S2. Desorption and absorption profiles for Excellion-Membrane.

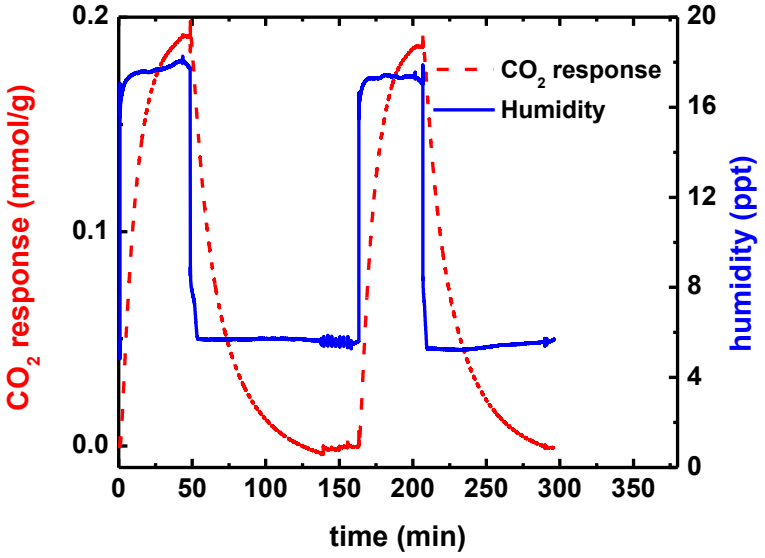

Figure S3. Desorption and absorption profiles for Excellion-Active Resin.

When the carbon black grafted material is subjected to similar conditions, there is an improvement in the kinetics. The desorption and absorption traces are shown in Figure S4 with an absorption rate of 1.8 $\times 10^{-2}$ mmol/g/min, a desorption rate of 1.2 $\times 10^{-2}$ mmol/g/min and a swing size of 1.4 $\times 10^{-1}$ mmol/g.

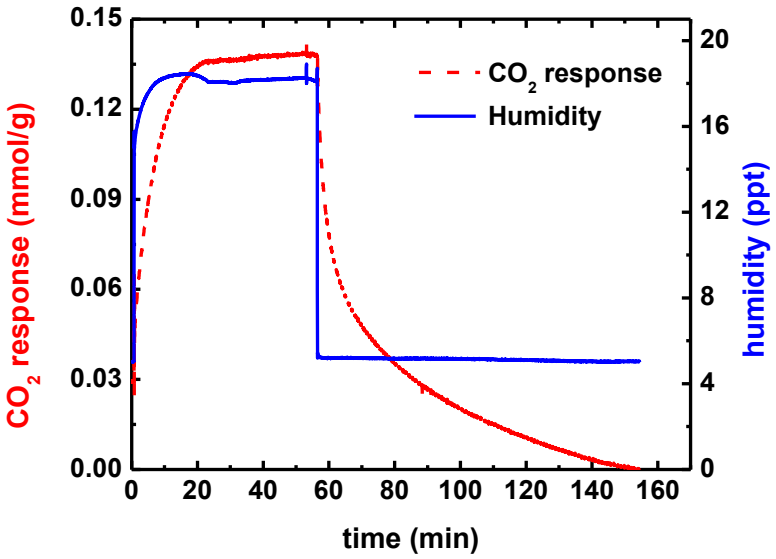

Figure S4. Desorption and absorption profiles for the carbon black grafted material.

The templated materials showed significantly improved kinetics and performance when compared to the previously analyzed materials. In particular the colloidal crystal templated material showed significantly better performance than the previously analyzed materials as seen in Figure S5. The colloidal crystal templated p(NR_3^+-MS OH^-) showed an absorption rate of 2.8 $\times 10^{-2}$ mmol/g/min, a desorption rate of 1.8 $\times 10^{-2}$ mmol/g/min and a swing size of 3.7 $\times 10^{-1}$ mmol/g.

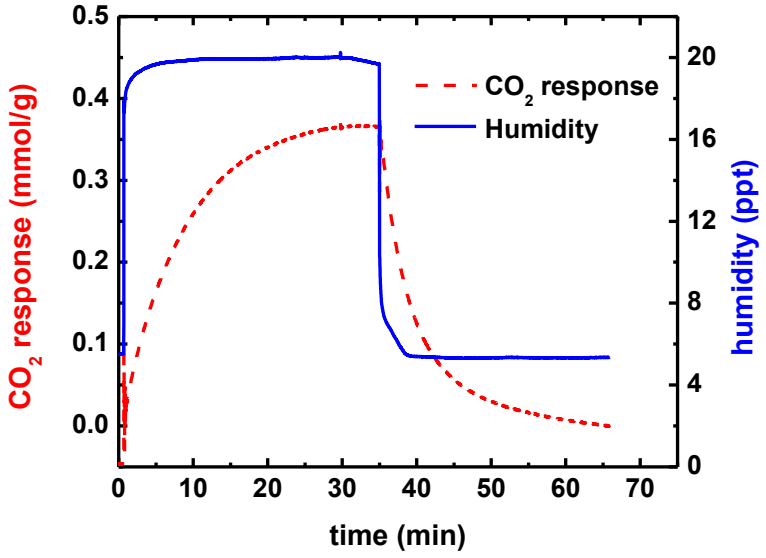

Figure S5. Desorption and absorption profiles for the colloidal crystal templated material.

Finally the HIPE based materials showed similar performance to the colloidal crystal templated material, although with faster kinetics. This is shown in Figure S6. The HIPE templated p(NR_3^+-MS OH^-) material had an absorption rate of 1.1×10^{-1} mmol/g/min, a desorption rate of 3.3×10^{-2} mmol/g/min and a swing size of 4.9×10^{-1} mmol/g.

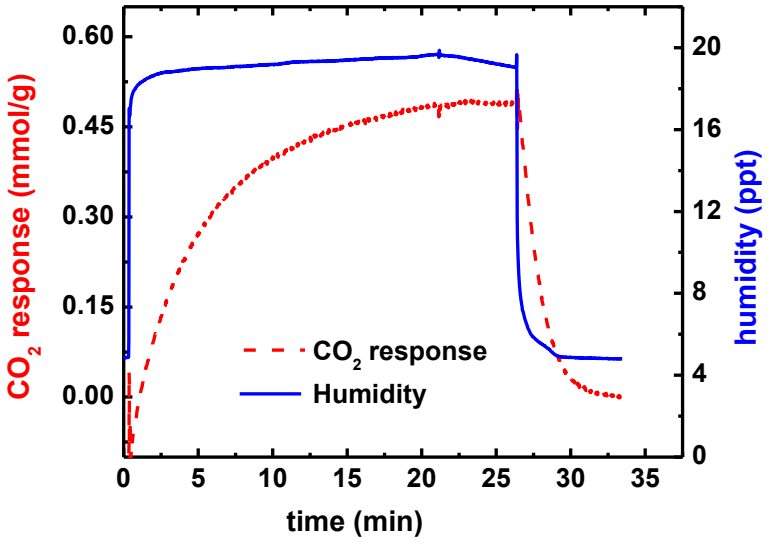

Figure S6. Desorption and absorption profiles for the HIPE based material.

With the measured swing size of 0.49 mmol/g, 5 mg of the HIPE material can change the concentration of CO_2 in a 100 mL chamber at 290 K from 400 ppm with the resin fully loaded with CO_2 to 980 ppm with the maximum amount of CO_2 released. In contrast, with the measured swing size of 0.13 mmol/g, 5 mg of the fully loaded Excellion membrane is only capable of changing the CO_2 concentration from 400 ppm to 550 ppm, under the same conditions. This implies that 5 mg of the HIPE based material can alter the CO_2 concentration in a sealed chamber of 100 mL by 150%, whereas 5 mg of the Excellion membrane is only capable of changing the concentration by 40%.

NMe_3^+-MS OH^- contents in Excellion membrane, Excellion active resin, carbon black grafted material, colloidal crystal templated material, and HIPE templated material.

The content of NMe_3^+-MS OH^- in the Excellion membrane and the Excellion active resin were estimated from the ion exchange capacity of the membrane of *ca.* 700 mmol/m^2.[8] In the case of the polymer grafted from carbon black, the polymer templated by colloidal crystal, and the polymer templated by HIPE, the NMe_3^+-MS OH^- content was found from the elemental analysis, as shown in Table S1.

The content of NMe_3^+-MS OH^- in Excellion membrane and Excellion active resin:

The NMe_3^+-MS Cl^- content of the of the Excellion membrane was determined from the capacity of *ca.* 700 mmol/m^2 before ion exchange, using the membrane thickness of 0.33 mm and a density of 0.98 g/cm^3.[8] This gives a mass per area of *ca.* 320 g/m^2, and using the capacity of *ca.* 700 mmol/m^2,[8] the NMe_3^+-MS OH^- content is *ca.* 700 mmol/m^2 ÷ 320 g/m^2 = 2.2 mmol/g, with full exchange of Cl^- to OH^-. Since titrations showed that the Excellion membrane was 50% polypropylene and 50% Excellion active resin, the NMe_3^+-MS OH^- content of the Excellion active resin was found to be *ca.* 4.4 mmol/g. This assumes a dry material for both the Excellion membrane and the Excellion active material.

The content of NMe_3^+-MS OH^- in CB-g-p(NMe_3^+-MS OH^-):

The Br content in CB-N-Br was 14.74 wt%, determined from the elemental analysis, which corresponds to 1.84 mmol/g. Thus, the N content (from the initiators on the CB-N-Br) was also 1.84 mmol/g. Thermogravimetric analysis (TGA) showed that the polymer represented 52.3 wt% of CB-*g*-CMS, so 1 g of CB-*g*-CMS contained 0.523 g of polymer and 0.477 g of CB-N-Br (containing 0.878 mmol of N). After converting from CB-*g*-CMS to CB-*g*-p(NMe_3^+-MS OH^-), the polymer represented *ca.* 58.2 wt% of CB-*g*-p(NMe_3^+-MS OH^-). Therefore, 1 g of CB-*g*-p(NMe_3^+-MS OH^-) contained 0.0489 g (or 3.493 mmol) of N determined by elemental analysis, and it also contained 0.418 g of CB-N-Br (with 0.769 mmol of N), so the N content in p(NMe_3^+-MS OH^-) was 3.493 mmol - 0.769 mmol = 2.724 mmol. However, CB-*g*-p(NMe_3^+-MS OH^-) also contained 0.67 wt% of Cl determined by elemental analysis, so for 1 g of CB-*g*-p(NMe_3^+-MS OH^-), it contained 0.189 mmol of Cl. Therefore, the OH^- content was 2.724 mmol - 0.189 mmol = 2.535 mmol. Thus, the content of NMe_3^+-MS OH^- in CB-g-p(NMe_3^+-MS OH^-) was *ca.* 2.5 mmol/g.

The content of NMe_3^+-MS OH^- in colloidal crystal templated material:

1 g of the colloidal crystal templated material contained 0.0456 g (or 3.257 mmol) of N determined by elemental analysis, and it also contained 0.033 g (or 0.930 mmol) of Cl determined by elemental analysis. Therefore, the OH^- contents was 3.257 mmol - 0.930 mmol = 2.327 mmol. Thus, the content of NMe_3^+-MS OH^- in colloidal crystal templated material was *ca.* 2.3 mmol/g.

The content of NMe_3^+-MS OH^- in HIPE templated material:

1 g of HIPE templated material contains 0.0366 g (or 2.614 mmol) of N determined by elemental analysis, and it contained no Cl determined by elemental analysis. Therefore, the OH^- contents was 2.614 mmol. Thus, the content of NMe_3^+-MS OH^- of the HIPE templated material was *ca.* 2.6 mmol/g.

Table S1. Elemental analysis for three advanced materials synthesized. Each material is a polyelectrolyte with quaternary ammonium ions attached to the polymer, and hydroxide counterions. The three materials are the polymer grafted from carbon black, the polymer templated by a colloidal crystal, and the polymer templated by a HIPE. The content of NMe_3^+-MS OH^- in Excellion membrane and Excellion active resin were *ca.* 2.2 and 4.4 mmol/g, respectively.

Sample	%N	%O	%Cl	Content of NMe_3^+-MS OH^- (mmol/g)
Carbon Black Grafted Material	4.89	10.76	0.67	2.5
Colloidal Crystal Templated Material	4.56	23.09	3.30	2.3
HIPE Templated Material	3.66	23.60	Not detected	2.6

TEM images of raw carbon black and carbon black grafted material

The carbon black grafted material and the raw carbon black were analyzed by TEM. As shown in Figure S7 (A), the raw carbon black forms aggregates and is poorly dispersed. On the other hand the functionalized carbon black (Figure S7 (B)) is well dispersed.

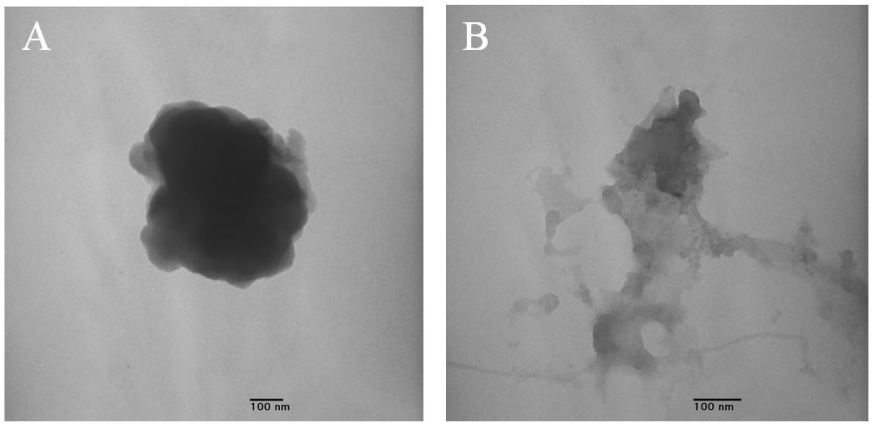

Figure S7. TEM images of raw carbon black (A) and functionalized carbon black (B).

SEM images of colloidal crystal, and porous material based on the colloidal crystal template

The SEM images of the colloidal crystal (Figure S8 (A and B)) and the size distribution (Figure S8 (C)). They show the regular packing of the colloidal crystal, and the narrow distribution of the particle sizes respectively. After the removal of the template, a well connected stable honeycomb-like structure results (Figure S8 (D)).

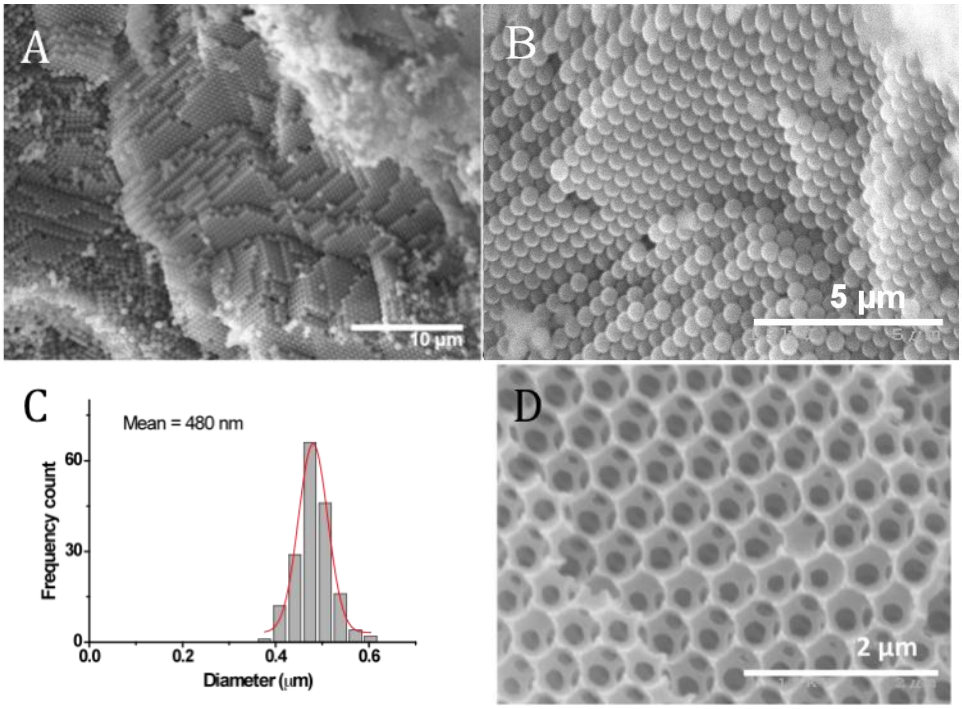

Figure S8. SEM images of PMMA colloidal crystals (A and B), size distribution (C) and the honeycomb material based on the colloidal crystal template (D).

XRM images of colloidal crystal templated materials

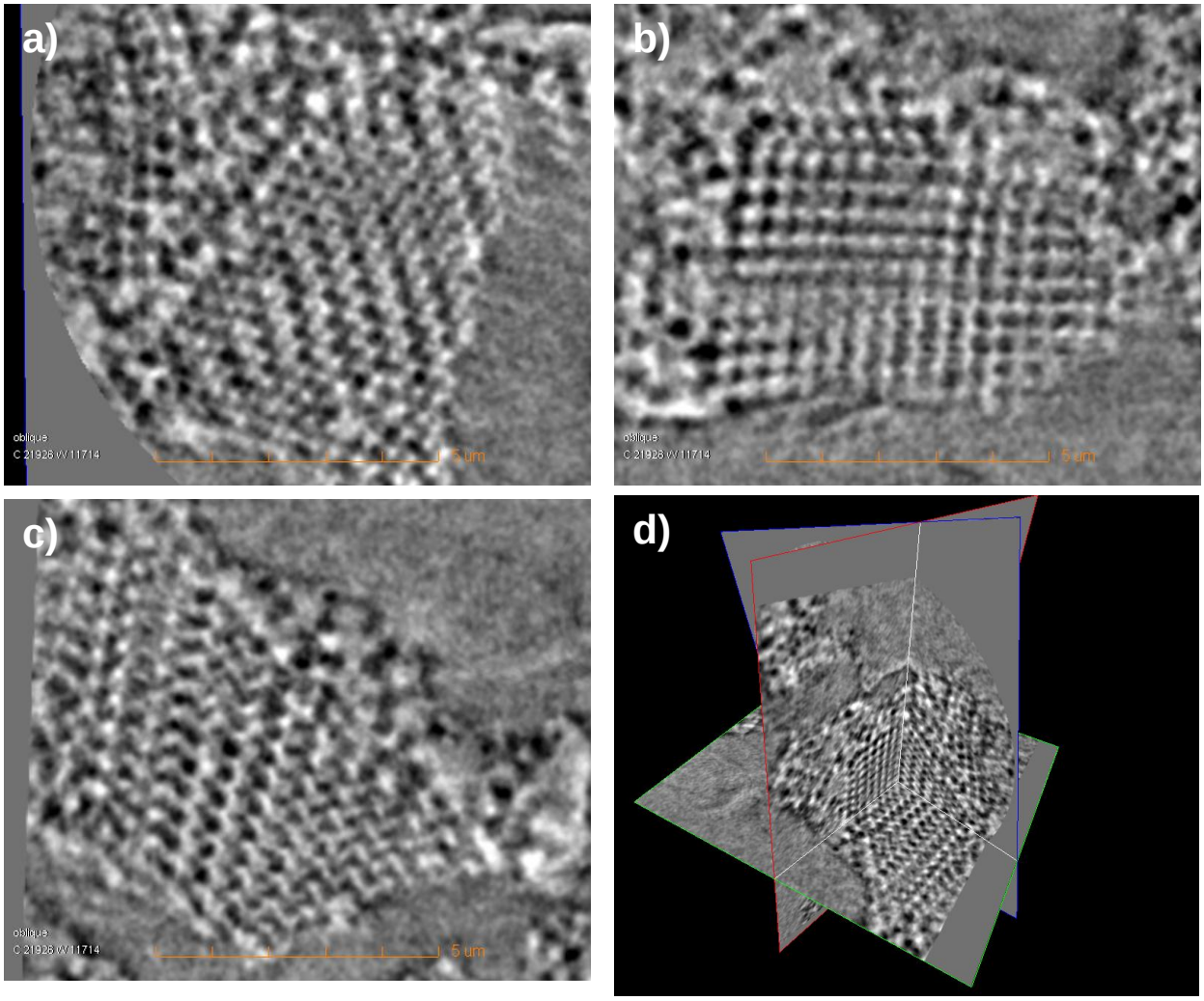

Figure S9. The nanoscale 3D XRM images of colloidal crystal templated p(NMe_3^+-MS OH^-) materials: (a-c) the virtual 2D slices through the 3D imaging volume, (d) the intersection between virtual slice viewing planes.

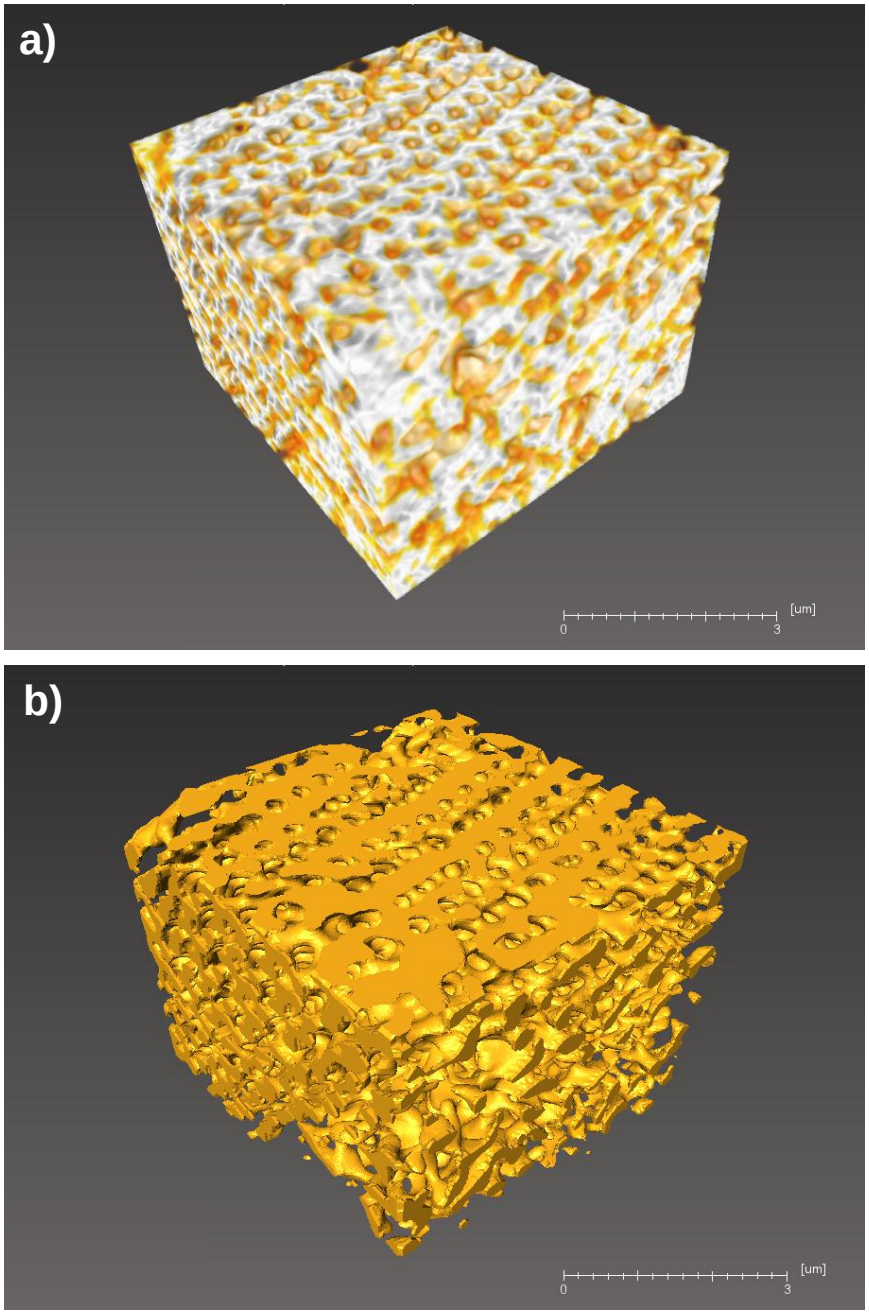

Figure S10. The nanoscale 3D XRM images of colloidal crystal templated p(NMe_3^+-MS OH^-) materials: visualization with Avizo® Fire(Visualization Sciences Group, Bordeaux, France) (a), and surface rendering of segmented strut network (b).

SEM images of unfunctionalized HIPE material

The SEM images of the unfunctionalized HIPE material are shown in Figure S11 (a,b), which show the highly porous structure of the material.

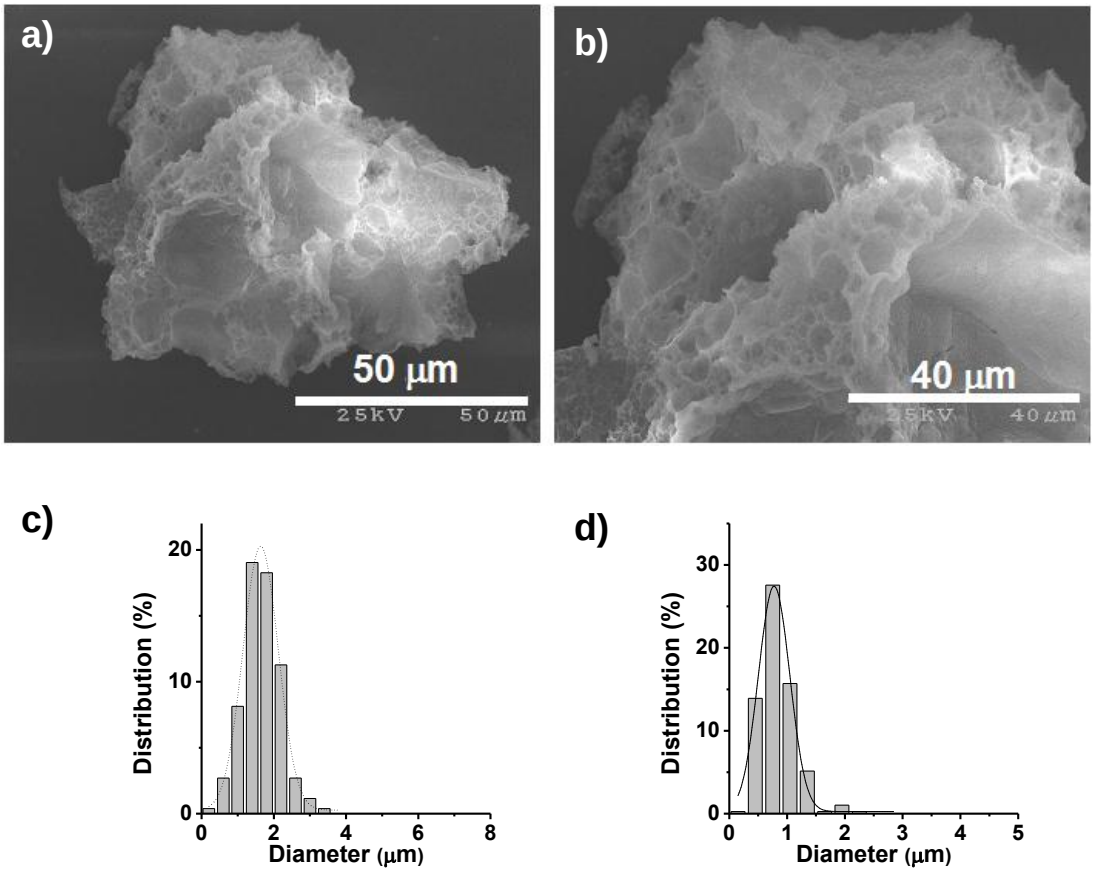

Figure S11. SEM images of HIPE material before functionalization (a,b), and the size distributions of the HIPE materials before (c) and after (d) functionalization The average pore sizes of the HIPE materials before and after functionalization are 1.65 and 0.83 μm, respectively.

a)

Carbon Cycle in Green Leaf

Photosynthesis

$$6CO_2 + 6H_2O \rightleftharpoons C_6H_{12}O_6 + 6O_2$$

Metabolism

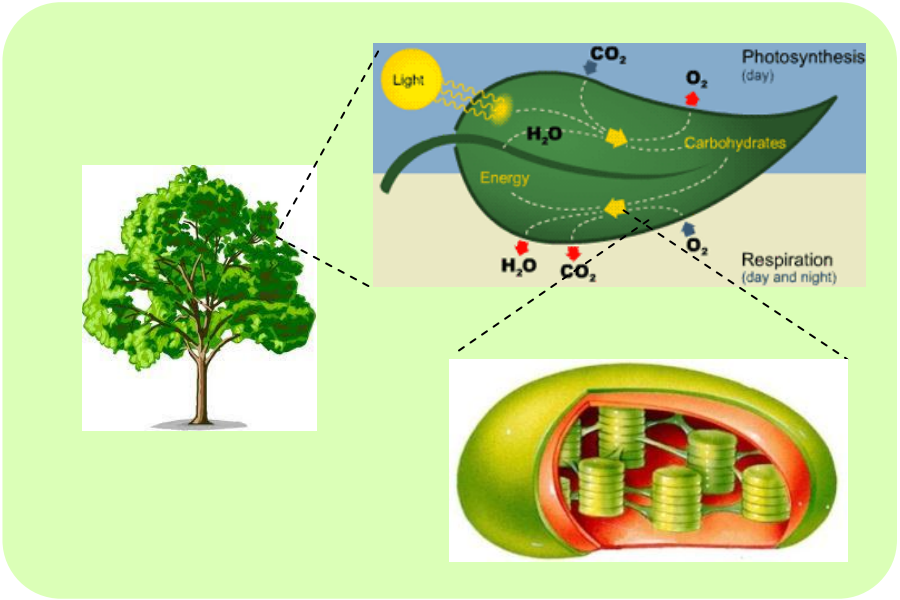

b)

Carbon Cycle in Red Blood Cell

Carbonic Anhydrases

$$CO_2 + H_2O \rightleftharpoons HCO_3^- + H^+$$

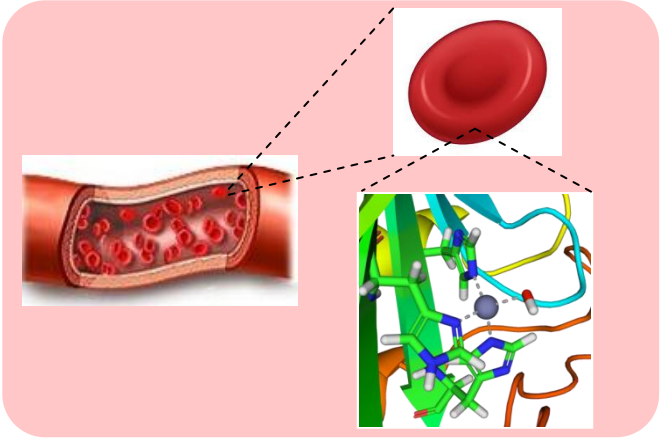

Scheme S2. The schematic illustration of the carbon cycles in (a) green leaf and (b) red blood cell. The chloroplasts in leaves are the most active photosynthetic organelles for CO_2 fixation of green plants. In chloroplasts, the thylakoids with a flattened disk shape are arranged in stacks of lamellar structures called grana. Photosynthesis takes place in the system of interconnecting flattened membrane compartments of the thylakoids.[9-10] In human bodies, the CO_2 capture and transport occurs in the red blood cells in the presence of the enzyme of carbonic anhydrases. The pocket structures of human carbonic anhydrase II (HCA2) play an integral role in the catalytic mechanism, and the binding of CO_2 to the active site of HCA2 is related with the optimal orientation of the substrate for nucleophilic attack by the zinc-bound hydroxide.[11-12]

Supplementary Videos

Video S1. The nanoscale 3D XRM movie of colloidal crystal templated materials (50 nm resolution utilizing Zernike phase contrast).

Video S2. The nanoscale 3D XRM movie of colloidal crystal templated materials (50 nm resolution utilizing Zernike phase contrast, shaded volume rendering technique).

Video S3. The nanoscale 3D XRM movie of colloidal crystal templated materials (50 nm resolution utilizing Zernike phase contrast, virtual slices).

Supplementary References

1. Wang, T.; Lackner, K. S.; Wright, A. *Environ. Sci. Technol.* **2011,** *45*, 6670-6675.
2. Pyun, J.; Jia, S.; Kowalewski, T.; Patterson, G. D.; Matyjaszewski, K. *Macromolecules* **2003,** *36*, 5094-5104.
3. Tkachuk, A.; Duewer, F.; Cui, H.; Feser, M.; Wang, S.; Yun, W. *Z. Kristallogr.* **2007,** *222*, 650-655.
4. Williamson, K. S.; Yoon, T. P. *J. Am. Chem. Soc.* **2010,** *132*, 4570-4571.
5. Sanseverino, A. M.; de Mattos, M. C. S. *J. Brazil. Chem. Soc.* **2001,** *12*, 685-687.
6. Wang, Z.; Kiesel, E. R.; Stein, A. *J. Mater. Chem.* **2008,** *18*, 2194-2200.
7. Zou, D.; Ma, S.; Guan, R.; Park, M.; Sun, L.; Aklonis, J. J.; Salovey, R. *J. Polym. Sci., Part B: Polym. Phys.* **1992,** *30*, 137-144.
8. SnowPure Excellion Ion Exchange Membranes. http://www.snowpure.com/docs/Excellion_Specifications_2011.pdf.
9. Adir, N.; Zer, H.; Shochat, S.; Ohad, I. *Photosynth. Res.* **2003,** *76*, 343-370.
10. Staehelin, L. A. *Photosynth. Res.* **2003,** *76*, 185-196.
11. Domsic, J. F.; Avvaru, B. S.; Kim, C. U.; Gruner, S. M.; Agbandje-McKenna, M.; Silverman, D. N.; McKenna, R. *J. Biol. Chem.* **2008,** *283*, 30766-30771.
12. Liang, J. Y.; Lipscomb, W. N. *Proc. Nat. Acad. Sci. USA* **1990,** *87*, 3675-3679.